Journal of
Mechanics of
Materials and Structures

SEISMIC VULNERABILITY OF DOMES: A CASE STUDY

Concetta Cusano, Claudia Cennamo and Maurizio Angelillo

Volume 13, No. 5 December 2018

msp

JOURNAL OF MECHANICS OF MATERIALS AND STRUCTURES
Vol. 13, No. 5, 2018
dx.doi.org/10.2140/jomms.2018.13.679

SEISMIC VULNERABILITY OF DOMES: A CASE STUDY

CONCETTA CUSANO, CLAUDIA CENNAMO AND MAURIZIO ANGELILLO

In this work, a simplified structural analysis of the main dome of San Francesco di Paola in Naples is performed by adopting both analytical and graphical approaches. The analytical process is based on the simplified membrane theory and the graphical methodology on the slicing technique. Both methods are used to determine the safety of the dome design under vertical and horizontal loads. We explore the effects of earthquakes by introducing horizontal forces proportional to the weight. Since the slicing technique does not consider the hoop compressive stresses building up in the upper part of the cap, the geometrical safety factor obtained by combining the analytical with the graphical method for the sole dome is lower than the one obtained with the analytical method. The estimate of the a/g factor for the dome-buttress structural system obtained with the graphical method is greater than the level accepted for the seismic area of Naples.

1. Introduction

The aim of the present work is to compare results of equilibrium analyses of masonry domes, treated as composed of Heyman's unilateral material and performed with both analytical and graphical methods, for a case study. The analytical method is based on the simplified membrane theory for unilateral materials (see [Angelillo and Fortunato 2004]) and the graphical method on the so-called slicing technique (see [Heyman 1966]). The two methods can be both employed to assess the geometrical safety factor of domes under the effect of vertical and horizontal loads.

A number of studies on dome analysis, based on kinematical approaches and considering the effect of earthquakes through collapse mechanisms, can be found in the recent literature (see, for example, [Arcidiacono et al. 2015; Zuccaro et al. 2017; Casapulla et al. 2017]). Whilst the present study is focused on structures composed of unilateral material, the seismic Italian codes on the stress verification for structures, such as vaults and domes, refer to materials which can withstand both tension and compression.

The reliability of analyses based on unilateral models, and for which the safety of the structure depends mainly on shape rather than on strength, directly depends on correct geometrical reconstructions. Besides geometry, the knowledge of constructive features, such as masonry stone/brick texture, details concerning the double shell function, and detection of voids inside the wall are essential: the relation between the construction technique and structural behavior is a key point in a structural safety assessment (see [Cennamo et al. 2018b]). Therefore, our analysis has been deepened with the knowledge both on the material of the construction and on the history of the construction.

The stability of historical masonry structures, such as arches, vaults, and domes, is effectively visualized through funicular curves (that is thrust paths of internal forces) carrying the external loads. It is

Keywords: seismic vulnerability, masonry domes.

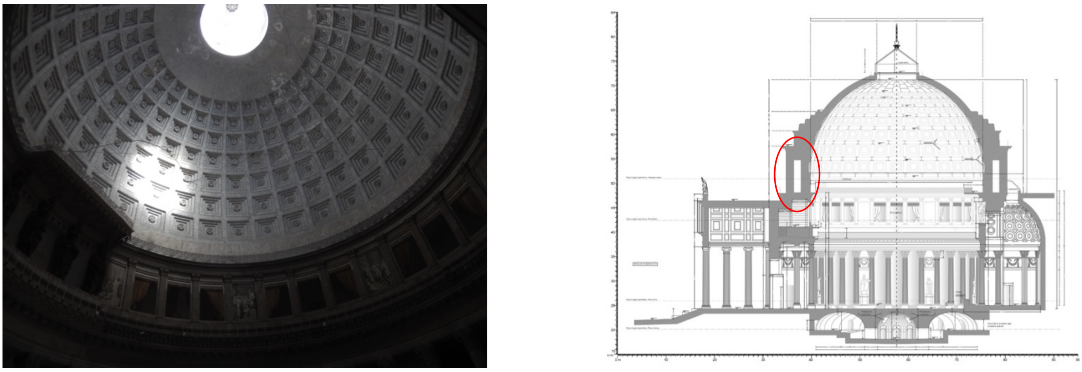

Figure 1. San Francesco di Paola in Naples: interior of the dome with coffers (left) and section of the Basilica by Tecno IN Geosolutions (right).

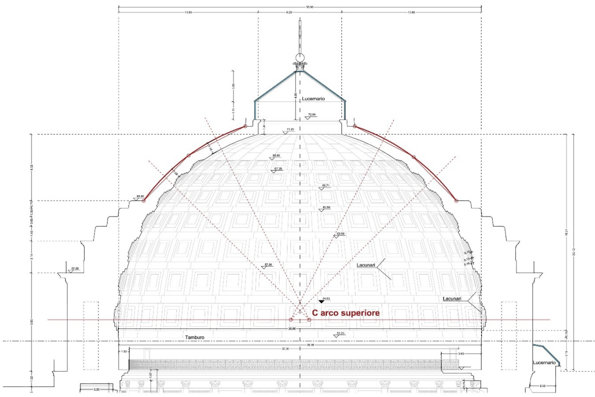

Figure 2. Drawing by the authors. Studies on the geometry of the dome.

their geometry that establishes the capacity to resist loads, both in statics and dynamics [Cennamo and Cusano 2018]. Masonry represents the typological opposite of buildings designed to cope with disasters [Cennamo et al. 2012] and yet, in practice, it often fares well in such emergencies, lasting centuries and millennia undamaged.

The method we propose to analyze domes is applied to a case study, the dome of San Francesco di Paola in Naples, a structural problem already laid out in [Cusano et al. 2017; Cennamo et al. 2017b].

From geognostic surveys carried out jointly with the Laboratory of the Department of Civil Engineering of the University of Salerno using GPR (ground penetrating radar), it can be seen that the brickwork is of good quality (that is, correctly toothed) and compact (that is, with no voids) [Cennamo et al. 2018b].

2. Seismic equivalent static analysis

The main load acting on a dome is the dead load due to the self-weight of the structure and of the superstructure; in normal conditions these loads act vertically.

The undulatory effect of the action of the earthquake ground motion, as a first approximation, can be represented by horizontal forces proportional to the weight. Then the direction of the loads become

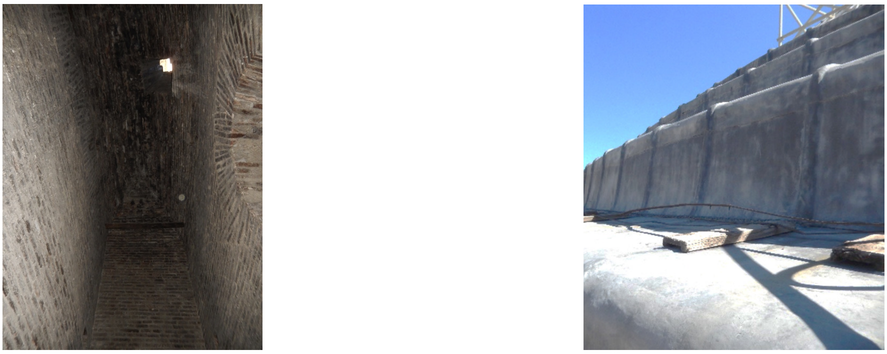

Figure 3. San Francesco di Paola in Naples: particular of the annular aisle in the drum (circled in red in Figure 1, right), whose structure is made of solid brick walls (left) and view of the upper surface of the dome covered with lead (right).

inclined with respect to the vertical: the slope of this direction, that is, the ratio between the horizontal and vertical components, is a measure, usually expressed in g, of the ground acceleration. The approximation inherent to the static approach is two-fold: it neglects both elastic deformation and wave propagation effects. Indeed, the main deformation of a masonry structure arises after a first phase of essentially uniform acceleration, when a mechanism is formed and the structure oscillates, essentially, as a one degree of freedom system. Besides the wave length of earthquake surface waves is at least two or three orders of magnitude bigger than the characteristic dimensions of any conventional masonry structure, that is, the effect of the soil movement is approximately uniform.

2.1. ***Slicing method.*** In order to analyze these three-dimensional structures with the slicing method [Cennamo et al. 2017b], the analyst slices the structure, reducing the 3D problem to a combination of 2D problems, for which the structural behavior becomes a combination of arch actions [Block and Ochsendorf 2008]. A dome can be cut with meridian planes, dividing it into arches: the stability condition (safe load theorem) states that a masonry dome which fulfills the theoretical assumptions of a limit analysis [Block and Ochsendorf 2008] is stable if a thrust line can be drawn within this arch section, that is, a possible equilibrium state of compression can be found. If this is the case, then the dome is safe, and will not collapse [Huerta 2001].

3. Case study

3.1. ***Graphical method.*** By adopting the slicing technique [Cennamo et al. 2017c], the dome has been divided into slices and the slices into ideal voussoirs. Figure 4 shows a generic slice of the dome, cut between two meridional planes.

With the graphical method, reported in Figure 5, the directions of the loads have been assumed with a slope of 10° with respect to the vertical axis. This corresponds to a value of $\lambda = a/g = 0.176$, a level of acceleration which is above the value of horizontal acceleration prescribed by the Italian regulations in the seismic area of Naples. As can be seen from Figure 5, by using the slicing method, such a level represents the maximum value of horizontal acceleration for which the thrust line can be entirely drawn within the masonry. Therefore, up to an inclination of the loads of 10°, as stated by the fundamental safe

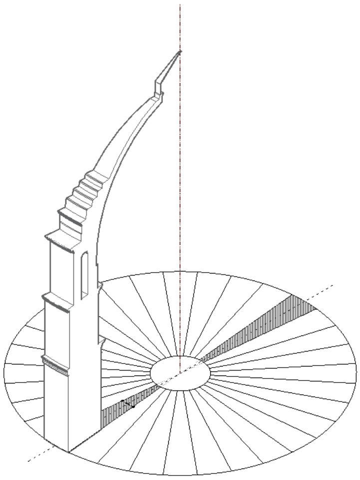

Figure 4. San Francesco di Paola in Naples. In order to study its stability, the dome has been divided into 32 spherical sectors.

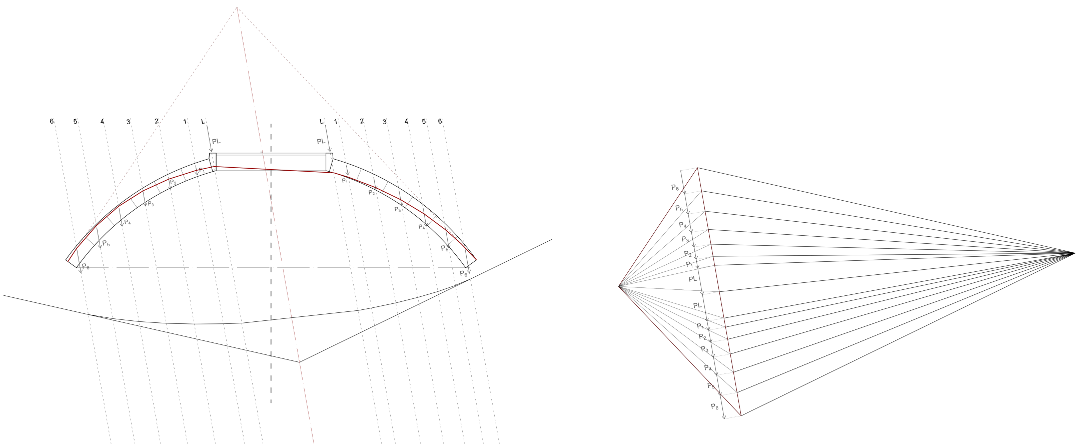

Figure 5. Graphical analysis with the loads inclined of 10°: calculation of the thrust line (left) and force diagram of the loads (right).

theorem [Cennamo et al. 2017b], the structure is stable and collapse cannot occur [Huerta 2004; Cusano et al. $\geq$ 2018].

The peak thrust force per unit length corresponding to $a = 0.176\,\mathrm{g}$ is $H = 304.73\,\mathrm{kN}$.

Stability of the buttress. The stability of the buttress is studied first by considering the element itself, without the effect of the thrust of the dome. The total weight of the buttress (1679230.11 kN) is applied in the centroid G of the element. The limit value of λ is then $\lambda^{\circ} = 0.30$ (see Figure 6, left). Considering the effect of the dome, the total force acting on the buttress is depicted in Figure 6, right. For such a force the limit value of λ is 0.175. Therefore, the whole system results in being stable with a value of 10° of inclination ($\lambda = 0.175$).

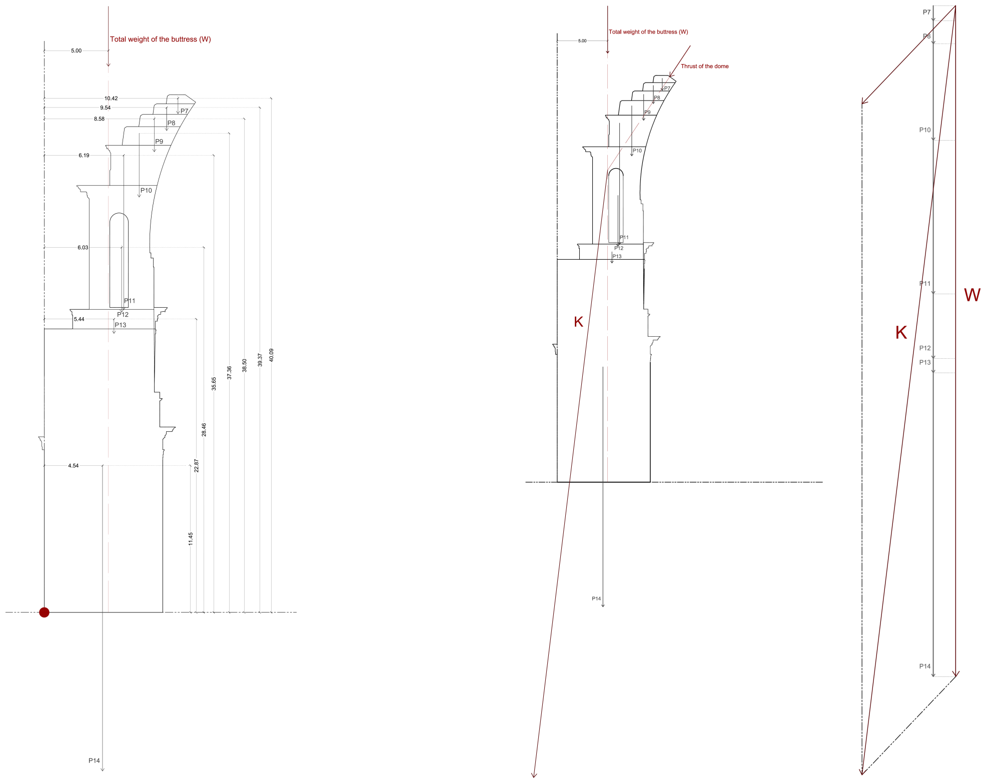

Figure 6. Left: total weight of the buttress and calculation of the limit value of λ without the effect of the thrust of the dome. Right: total force acting on the buttress considering the effect of the dome. Note that the total weight of the buttress (W) is 1679230.11 kN, the thrust of the dome is 339676.96 kN, and the total thrust (K) is 1939734.25 kN.

3.2. ***Membrane analysis.*** In this section the equilibrium of the dome is studied with the thrust membrane analysis. The external load is considered lumped on a surface S internal to the masonry, as a distributed load per unit area. The internal stress is also lumped on the surface S, that is, as a generalized membrane stress per unit length concentrated on S.

Under these hypotheses, the equilibrium of the membrane S can be expressed in terms of projected stresses defined on the planform Ω of S [Pucher 1934; Angelillo and Fortunato 2004; Heyman 2012].

In a Cartesian reference $\{0;\ x_1, x_2, x_3\}$, with the planform Ω contained in the plane $\{0;\ x_1, x_2\}$, the basic differential equation which rules the equilibrium of the membrane S, written in terms of projected Cartesian stress components $S_{\alpha\beta}$ (the shades of the actual membrane stresses on the planform) with $\alpha, \beta \in \{1, 2\}$ is

$$S_{\alpha\beta} f_{,\alpha\beta} - p_\gamma f_{,\gamma} + p_3 = 0, \tag{1}$$

where p_1, p_2, p_3 are the components of the distributed weight per unit area, f charts the surface S in Monge description, and $f_{,\gamma}$, $f_{,\alpha\beta}$, are the components of the gradient and of the Hessian of f.

When forces stand parallel to the axis x_3, then $p_1 = 0$, $p_2 = 0$, and the obtained stresses can be expressed in terms of an Airy's stress potential F:

$$S_{11} = F_{,22}, \quad S_{22} = F_{,11}, \quad S_{12} = S_{21} = -F_{,12}. \tag{2}$$

From (2), it is possible to rewrite the transverse equilibrium equation in the form

$$F_{,22} f_{,11} + F_{,22} f_{,11} - 2F_{,12} f_{,12} - p = 0, \tag{3}$$

where $p = -p_3$. If proper boundary conditions are prescribed at the boundary of Ω, the second order partial differential equation for the stress function F can be solved univocally. To ensure that the dome is in a compression state, the stress function F must be concave (the Hessian of F must be negative semidefinite) and the surface S must be contained within the masonry. In the present study, a convenient form f has been fixed inside the dome and, by solving numerically the transverse equilibrium equation, the corresponding stress F has been found.

By using cylindrical curvilinear coordinates $\{\rho, \vartheta, z\}$, relations (2) and (3) can be rewritten in the forms

$$S_{\rho\rho} = \frac{1}{\rho} F_{,\rho} + \frac{1}{\rho^2} F_{,\vartheta\vartheta}, \quad S_{\vartheta\vartheta} = R_{,\rho\rho}, \quad S_{12} = S_{21} = -\Big(\frac{1}{\rho} F_{,\vartheta}\Big), \tag{4}$$

$$\Big(\frac{1}{\rho} F_{,\rho} + \frac{1}{\rho^2} F_{,\rho\rho}\Big) f_{,\rho\rho} + F_{,\rho\rho}\Big(\frac{1}{\rho} f_{,\rho} + \frac{1}{\rho^2} f_{,\vartheta\vartheta}\Big) - 2\Big(\frac{1}{\rho} F_{,\vartheta}\Big)_{,\rho}\Big(\frac{1}{\rho} f_{,\vartheta}\Big)_{,\rho} - p = 0. \tag{5}$$

In the particular case in which axial symmetry of the load and of the boundary conditions is present, the *functions* F, f depend on ρ only, and (4), (5) reduce to the simple forms

$$S_{\rho\rho} = \frac{1}{\rho} F_{,\rho}, \quad S_{\vartheta\vartheta} = F_{,\rho\rho}, \quad S_{12} = S_{21} = 0, \tag{6}$$

$$\Big(\frac{1}{\rho} F_{,\rho}\Big) f_{,\rho\rho} + F_{,\rho\rho}\Big(\frac{1}{\rho} f_{,\rho}\Big) - p = 0. \tag{7}$$

The transverse equilibrium equation (7) can be easily solved numerically after becoming an ordinary differential equation for F.

By making the aforesaid simplifications on the effect of the seismic actions, that is, by considering that the structure is rigid and is rigidly connected to the soil, calling ρ the mass density of the material and a the given acceleration of the soil, the body load per unit volume acting on the structure consists of a vertical component ρg and of a horizontal component ρa. It is possible to estimate the level of ground acceleration that the structure can sustain by considering increasing values of the horizontal load component and by detecting, for any such value, a stress regime that is balanced with the loads and within the limits of the material [De Piano et al. 2017; Cennamo and Fiore 2013].

When reaching its limit horizontal acceleration, the structure forms a mechanism composed of rigid blocks articulated among each other, and a dynamic motion of the structure, different from that of the soil, begins. In the present paper, the study is restricted to the dynamic phase which precedes the formation of such a mechanism.

3.3. ***Vertical and slanted loads.*** Considering a horizontal component ρa *of the given forces*, the loads are no longer purely vertical and axial symmetry relative to the z axis is lost, but the loads can be

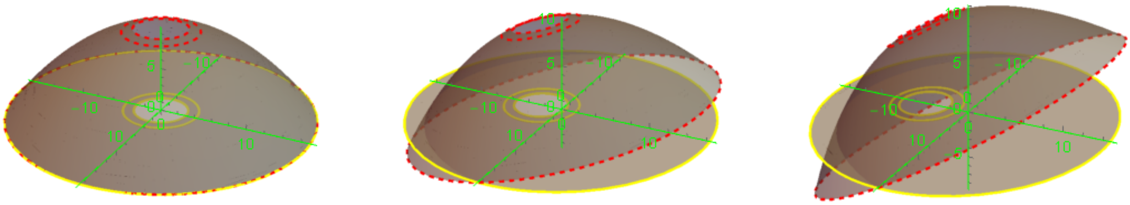

Figure 7. Rotated shapes for $a = 0.000\,\mathrm{g}$, $\alpha = 0°$ (left); $a = 0.268\,\mathrm{g}$, $\alpha = 15°$ (middle); and $a = 0.577\,\mathrm{g}$, $\alpha = 30°$ (right).

approximated as parallel; thus, the dome equilibrium can be given again by (8), rewritten in a Cartesian reference system in which the axes z and y are rotated about the x axis of an angle $\alpha = \arctan(a/g)$.

On the plane of the rotated axes x, y, the planform Ω becomes the projection in the rotated z direction of the ring of internal radius $r_i = 4.20\,\mathrm{m}$ and external radius $r_e = 16.95\,\mathrm{m}$.

The transverse equilibrium equation (that is, a second-order PDE in the unknown scalar function F) is rewritten below in Cartesian:

$$F_{,22} f_{,11} + F_{,22} f_{,11} - 2F_{,12} f_{,12} - p = 0. \tag{8}$$

Such a differential equation for F, approximated variationally, is solved numerically with the package for approximate PDE solutions in the program Mathematica.

Taking into account that in the case of a dome with an oculus where the stress must be zero at the internal rim, the boundary conditions are two: the first of Dirichelet type ($F = 0$), and the second of Neumann type ($dF/dn = 0$), both prescribed at the internal boundary. Consequently, an iterative shooting method has been adopted to solve the problem by imposing boundary conditions in the form of a Neumann homogeneous condition at the internal rim and of a sequence of Dirichelet boundary conditions at the external boundary, until the value of F at the internal boundary was approximately zero. In the analysis, three values of $a = \lambda g$, and the corresponding angles of rotation $\alpha = \arctan(\lambda)$, have been considered:

$$a = 0.000\,\mathrm{g}, \quad \alpha = 0°,$$
$$a = 0.268\,\mathrm{g}, \quad \alpha = 15°,$$
$$a = 0.577\,\mathrm{g}, \quad \alpha = 30°.$$

In the first case the loads are vertical.

Figure 7 illustrates the rotated shapes, corresponding to the three analyzed cases, and the corresponding distributed loads per unit projected area.

In Figure 8, the shape adopted for the membrane and a comparison of the shape of the membrane with the extrados and intrados surfaces in a axial section of the dome are shown in Figure 8.

In Figure 9, the solutions for the three cases in terms of stress potential are shown as 3D plots.

Note that, with the maximal horizontal acceleration that we consider $a = 0.577\,\mathrm{g}$, small tractions begin to appear along the "upwind" side of the outer boundary. These tensile stresses could be easily removed by concavifying a small part of the stress surface F, and adapting the membrane surface at the same location, by solving (8) for f.

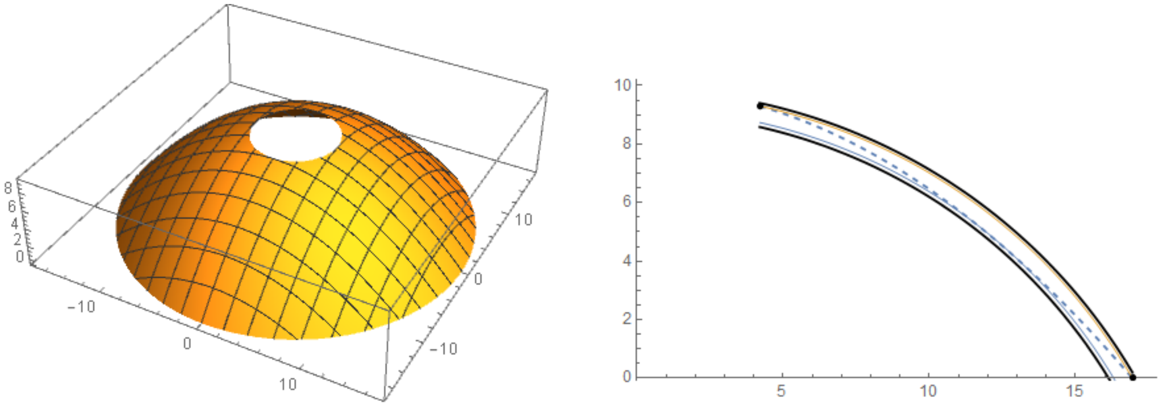

Figure 8. Paraboloid S: sections (left) and membrane surface (dotted), extrados and intrados surfaces (thick lines, right); the light gray lines denote the traces of the spheres tangent to the paraboloid.

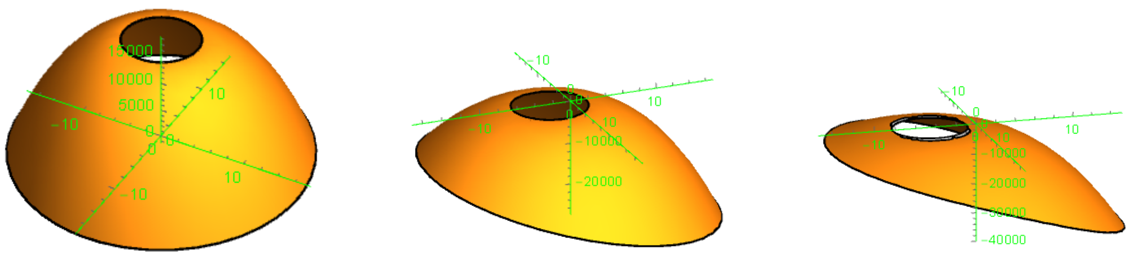

Figure 9. 3D plots of the stress function for the three cases: $a = 0.000\,\mathrm{g}$, $\alpha = 0°$ (left); $a = 0.268\,\mathrm{g}$, $\alpha = 15°$ (middle); and $a = 0.577\,\mathrm{g}$, $\alpha = 30°$ (right).

	$a = 0.000\,\mathrm{g}$	$a = 0.268\,\mathrm{g}$	$a = 0.577\,\mathrm{g}$
H	175.4 kN/m	245.7 kN/m	334.1 kN/m
$\sigma_{\max}$	0.375 MPa	0.416 MPa	0.545 MPa

Table 1. Maximum thrust force per unit length and maximum negative stress.

The stress state represented in Figure 9 (right) can be accepted as statically admissible. In Table 1, the estimates of the peak thrust force per unit length H and of the maximum negative stress $\sigma_{\max}$, obtained in the three cases, are reported.

The level lines of the maximal and minimal principal stresses and the isostatic lines are reported in Figure 10 for the three cases.

The graphical analysis performed in Section 3.1 shows that the value $\lambda = 0.176$ is already at the limit state of rocking for the buttress (see Figure 6). Therefore, this improved value of the horizontal force multiplier is actually ineffective with regards to the stability of the dome-buttress aggregate.

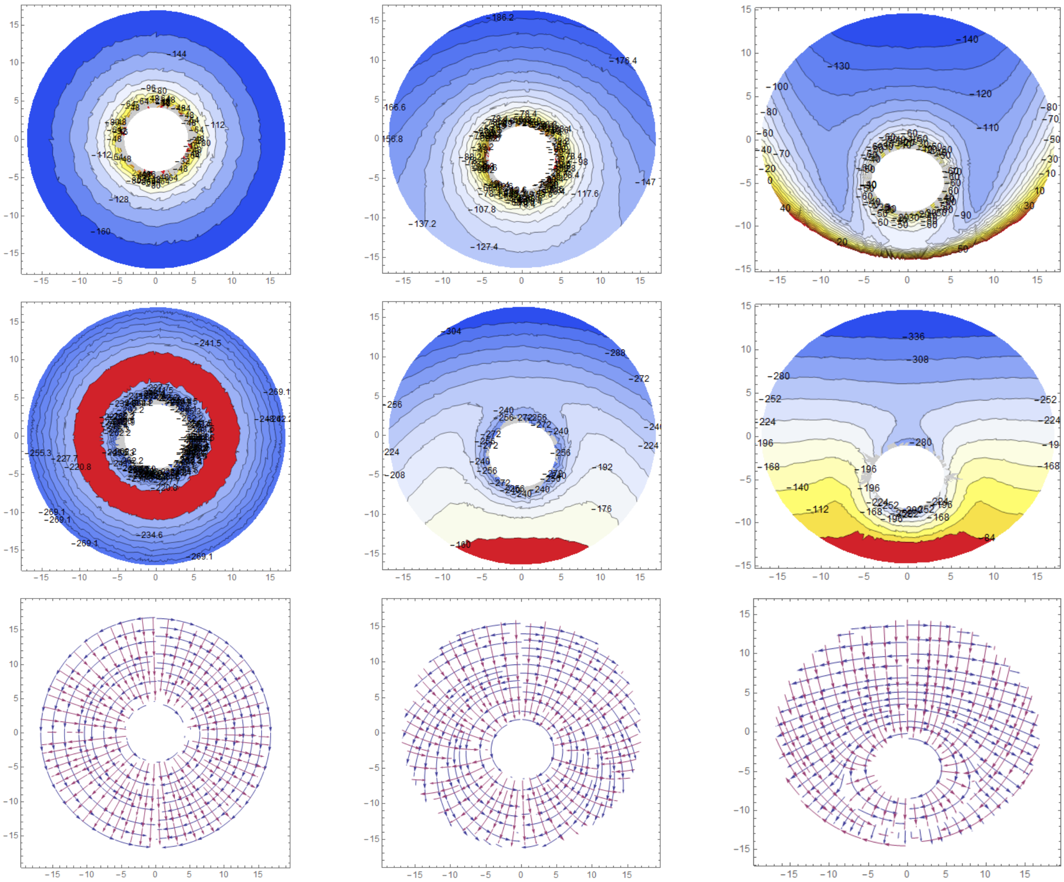

Figure 10. Level curves of the maximal and minimal normal stresses and isostatic lines trajectories for the three cases: $a = 0.000\,\mathrm{g}$, $\alpha = 0°$ (left column); $a = 0.268\,\mathrm{g}$, $\alpha = 15°$ (middle column); and $a = 0.577\,\mathrm{g}$, $\alpha = 30°$ (right column).

4. Conclusions

In a recent work on the Dome of San Francesco di Paola by the same authors (see [Cennamo et al. 2017a; 2018a]) the stability of the dome under vertical loads was discussed by using both the kinematic theorem and the safe theorem of limit analysis.

The aim of this further study is to assess the stability under horizontal actions. The horizontal force capacity of the dome-buttress system can be evaluated through a tilting test, that is, by rotating the structure about a horizontal axis (say the y axis) until the collapse load is reached. The aim of the present work is to determine the limit value of the dome inclination for which the masonry is still entirely compressed, and to assess the buttress stability.

The tilting test was simulated by rotating the body forces of an angle α and studying first the effect of tilting on the sole dome with two different methods, the graphical "slicing" method and the thrust membrane analysis, obtaining with the first method a limit value of $\alpha = 10°$, and with the second method of $\alpha = 30°$.

By considering the effect of tilting on the dome-buttress structural system, the whole system results in stable up to a value of 10° of inclination. This value corresponds to a value of a/g of 0.175 which is above the value of ground acceleration prescribed by the seismic regulation for the zone of the historical center of Napoli.

References

[Angelillo and Fortunato 2004] M. Angelillo and A. Fortunato, "Equilibrium of masonry vaults", pp. 105–111 in *Novel approaches in civil engineering*, edited by M. Frémond and F. Maceri, Lect. Notes Appl. Comput. Mech. **14**, Springer, 2004.

[Arcidiacono et al. 2015] V. Arcidiacono, G. P. Cimellaro, and J. A. Ochsendorf, "Analysis of the failure mechanisms of the basilica of Santa Maria di Collemaggio during 2009 L'Aquila earthquake", *Eng. Struct.* **99** (2015), 502–516.

[Block and Ochsendorf 2008] P. Block and J. Ochsendorf, "Lower-bound analysis of masonry vaults", pp. 593–600 in *Structural analysis of historic construction* (Bath, UK, 2008), edited by D. D'Ayala and E. Fodde, Proc. Int. Conf. Structural Anal. Historical Constructions **6**, CRC Press, Boca Raton, 2008.

[Casapulla et al. 2017] C. Casapulla, A. Maione, and L. U. Argiento, "Seismic analysis of an existing masonry building according to the multi-level approach of the Italian guidelines on cultural heritage", *Ingegneria Sismica* **34**:1 (2017), 40–59.

[Cennamo and Cusano 2018] C. Cennamo and C. Cusano, "The gothic arcade of Santa Maria Incoronata in Naples: equilibrium of gothic arches", *Int. J. Masonry Res. Innov.* **3**:2 (2018), 92–107.

[Cennamo and Fiore 2013] C. Cennamo and M. D. Fiore, "Best practice of structural retrofit: the SS. Rosario Church in Gesualdo, Italy", *Int. J. Disaster Resilience in the Built Environment* **4** (2013), 215–235.

[Cennamo et al. 2012] C. Cennamo, G. M. Cennamo, and B. Chiaia, "Robustness-oriented design of a panel-based shelter system in critical sites", *J. Architect. Engin.* **18**:2 (2012), 123–139.

[Cennamo et al. 2017a] C. Cennamo, M. Angelillo, and C. Cusano, "Structural failures due to anthropogenic sinkholes in the urban area of Naples and the effect of a FRP retrofitting", *Compos. B Eng.* **108** (2017), 190–199.

[Cennamo et al. 2017b] C. Cennamo, C. Cusano, and M. Angelillo, "The neoclassical dome of San Francesco di Paola in Naples: a study on form and stability", pp. 1439–1448 in *Proc. 23rd Conf. Italian Association of Theoretical and Applied Mechanics* (Salerno, 2017), edited by L. Ascione et al., Univ. Salerno, 2017.

[Cennamo et al. 2017c] C. Cennamo, C. Cusano, and L. Guerriero, "The slicing technique for the evaluation of the formal efficiency: a comparative study", pp. 1543–1554 in *Proc. 23rd Conf. Italian Association of Theoretical and Applied Mechanics* (Salerno, 2017), edited by L. Ascione et al., Univ. Salerno, 2017.

[Cennamo et al. 2018a] C. Cennamo, C. Cusano, and M. Angelillo, "On the statics of large domes: a static and kinematic approach for San Francesco di Paola in Naples", pp. 504–517 in *Proc. 10th Int. Masonry Conference* (Milan, 2018), 2018.

[Cennamo et al. 2018b] C. Cennamo, C. Cusano, A. Fortunato, and M. Angelillo, "A study on form and seismic vulnerability of the dome of San Francesco di Paola in Naples", *Ingegneria Sismica* **35**:1 (2018), 88–108.

[Cusano et al. 2017] C. Cusano, C. Cennamo, and M. Angelillo, "Estabilidad en el neoclasico napolitano y vulnerabilidad sísmica de la cúpula de San Francisco de Paula [sic] en Nápoles", pp. 399–406 in *Congreso Internacional Hispanoamericano de Historia de la Construcción, II* (Donostia/San Sebastián, 2017), edited by S. Huerta et al., Inst. Juan de Herrera, Madrid, 2017.

[Cusano et al. $\geq$ 2018] C. Cusano, C. Cennamo, and M. Angelillo, "A limit analysis approach for masonry domes: the basilica of San Francesco di Paola in Naples", *Int. J. Masonry Res. Innov.* **4**:3, 227–242.

[De Piano et al. 2017] M. De Piano, M. Modano, G. Benzoni, V. P. Berardi, and F. Fraternali, "A numerical approach to the mechanical modeling of masonry vaults under seismic loading", *Ingegneria Sismica* **34**:4 (2017), 103–119.

[Heyman 1966] J. Heyman, "The stone skeleton", *Int. J. Solids Struct.* **2**:2 (1966), 249–279.

[Heyman 2012] J. Heyman, "The membrane analysis of thin masonry shells", pp. 281–290 in *Nuts & bolts of construction history: culture, technology and society* (Paris, 2012), edited by R. Carvais et al., Proc. Int. Congress on Construction History **4**, Picard, Paris, 2012.

[Huerta 2001] S. Huerta, "Mechanics of masonry vaults: the equilibrium approach", pp. 47–69 in *Historical constructions: possibilities of numerical and experimental techniques* (Guimarães, 2001), edited by P. B. Lourenço and P. Roca, Proc. Int. Conf. Structural Anal. Historical Constructions **3**, Univ. Minho, Guimarães, Portugal, 2001.

[Huerta 2004] S. Huerta, *Arcos, bóvedas y cúpulas: geometría y equilibrio en el cálculo tradicional de estructuras de fábrica*, Inst. Juan de Herrera, Madrid, 2004.

[Pucher 1934] A. Pucher, "Über der Spannungzustand in gekrümmten Flächen", *Beton Eisen* **33** (1934), 298–304.

[Zuccaro et al. 2017] G. Zuccaro, F. Dato, F. Cacace, D. D. De Gregorio, and S. Sessa, "Seismic collapse mechanisms analyses and masonry structures typologies: a possible correlation", *Ingegneria Sismica* **34**:4 (2017), 121–149.

Received 7 Aug 2018. Accepted 20 Aug 2018.

CONCETTA CUSANO: concetta.cusano@unicampania.it
Department of Architecture and Industrial Design, University of Campania "Luigi Vanvitelli", Aversa, Italy

CLAUDIA CENNAMO: claudia.cennamo@unicampania.it
Department of Architecture and Industrial Design, University of Campania "Luigi Vanvitelli", Aversa, Italy

MAURIZIO ANGELILLO: mangelillo@unisa.it
Dipartimento di Ingegneria Civile, Università degli Studi di Salerno, Fisciano, Italy

JOURNAL OF MECHANICS OF MATERIALS AND STRUCTURES

msp.org/jomms

Founded by Charles R. Steele and Marie-Louise Steele

Cover photo: Wikimedia Commons

See msp.org/jomms for submission guidelines.

JoMMS (ISSN 1559-3959) at Mathematical Sciences Publishers, 798 Evans Hall #6840, c/o University of California, Berkeley, CA 94720-3840, is published in 10 issues a year. The subscription price for 2018 is US $615/year for the electronic version, and $775/year (+$60, if shipping outside the US) for print and electronic. Subscriptions, requests for back issues, and changes of address should be sent to MSP.

JoMMS peer-review and production is managed by EditFlow® from Mathematical Sciences Publishers.

PUBLISHED BY
mathematical sciences publishers
nonprofit scientific publishing
http://msp.org/

Journal of Mechanics of Materials and Structures

Volume 13, No. 5 December 2018

Special issue on

Structural Analysis of Real Historic Buildings (part 1)